Bioorg. Med. Chem. Lett. 45 (2021) 128138

Contents lists available at ScienceDirect

Bioorganic & Medicinal Chemistry Letters

journal homepage: www.elsevier.com/locate/bmcl

Discovery of 3,4-dihydrobenzo[*f*][1,4]oxazepin-5(2*H*)-one derivatives as a new class of ROCK inhibitors for the treatment of glaucoma

Yumeng Sun [a,1], Yueshan Li [b,1], Zhuang Miao [b], Ruicheng Yang [b], Yun Zhang [b,c], Ming Wu [b], Guifeng Lin [b], Linli Li [a,*]

[a] *Key Laboratory of Drug Targeting and Drug Delivery System of Ministry of Education, West China School of Pharmacy, Sichuan University, Sichuan 610041, China*
[b] *State Key Laboratory of Biotherapy and Cancer Center, West China Hospital, Sichuan University, Chengdu, Sichuan 610041, China*
[c] *Macular Disease Research Laboratory, Department of Ophthalmology, West China Hospital, Sichuan University, Sichuan 610041, China*

ARTICLE INFO

Keywords:
ROCK inhibitors
Structure–activity relationship
Glaucoma
IOP-lowering effect

ABSTRACT

The Rho-associated protein kinases (ROCKs) are associated with the pathology of glaucoma and discovery of ROCK inhibitors has attracted much attention in recent years. Herein, we report a series of 3,4-dihydrobenzo[*f*][1,4]oxazepin-5(2*H*)-one derivatives as a new class of ROCK inhibitors. Structure-activity relationship studies led to the discovery of compound **12b**, which showed potent activities against ROCK I and ROCK II with IC_{50} values of 93 nM and 3 nM, respectively. **12b** also displayed considerable selectivity for ROCKs. The mean IOP-lowering effect of **12b** in an ocular normotensive model was 34.3%, and no obvious hyperemia was observed. Overall, this study provides a good starting point for ROCK-targeting drug discovery against glaucoma.

Glaucoma is one of the primary causes of blindness and the global number of patients with glaucoma is estimated to be more than 111.8 million in 2040.[1,2] Glaucoma patients often bear a combination of symptoms including elevated intraocular pressure (IOP), irreversible optic neuropathy and different degrees of corneal endothelial cell dysfunction until loss of visual field.[3–5] Lowing IOP is the most efficient strategy for the treatment of glaucoma.[6] Notably, each millimeter of mercury (mmHg) reduction in IOP, the risk of the glaucomatous field impairment progression can be decreased by 10–19% for glaucoma patients.[7]

Rho-associated protein kinases (ROCKs), which are widely expressed in the trabecular meshwork (TM), have been demonstrated to play an important role in the pathology of glaucoma.[8] After activation by Rho-GTPase, ROCK phosphorylate the intracellular downstream substrates,[9] such as myosin phosphatase targeting subunit 1 (MYPT1), myosin light chain (MLC), and LIM kinases (LIMK).[10–13] ROCK inhibitors have been demonstrated to be able to efficiently decrease IOP by acting on TM and altering the cytoskeleton.[14] Meanwhile, it also plays a role in optic nerve protection through increasing retinal vascular perfusion and promoting optic nerve regeneration.[15,16] Currently, a number of ROCK inhibitors have been reported to anti-glaucoma. Fig. 1 shows several representative examples, including ripasudil, netarsudil, Y-27632, Y-39983, SR-3677, INS117548.[7,15,17] Among them, ripasudil[18] and netarsudil,[19,20] have been approved to use clinically as anti-glaucoma drugs. Despite a good therapeutic effect, these two drugs show an adverse effect of conjunctival hyperemia, which could be due to the poor kinase selectivity.[1,21–24] Therefore, discovering more potent and selective ROCK inhibitors is necessary at present.

To identify new ROCK inhibitors, we screened our in-house chemical library containing about 1000 compounds synthesized by our group, which led to the retrieving of a ROCK inhibitor with a new scaffold 3,4-dihydroisoquinolin-1(2*H*)-one (**Hit 1**, Fig. 2). **Hit 1** is a dual ROCK I/II inhibitor with IC_{50} values of 2.062 ± 0.103 μM and 0.632 ± 0.059 μM, respectively. A further structural optimization was carried out in this investigation.

The structural optimization and SAR analyses were focused on three regions: 3,4-dihydroisoquinolin-1(2*H*)-one (region I), 1*H*-indazole (region II) and anisole (region III).

In the first step, we fixed region II and III, and varied region I. A total of four compounds (**6**, **10a-c**) were synthesized. As shown in Scheme 1, 3-methoxybenzylamine reacted with 4-bromo-2-hydroxybenzoyl chloride (**2**), which was prepared by refluxing reaction of 4-bromo-2-hydroxybenzoic acid (**1**) in $SOCl_2$, to generate intermediate **3**. Compound **4** was then obtained by cyclization from intermediate **3.** Suzuki-Miyaura

* Corresponding author.
E-mail address: lilinli@scu.edu.cn (L. Li).
[1] These authors contributed equally to this work.

https://doi.org/10.1016/j.bmcl.2021.128138
Received 5 February 2021; Received in revised form 16 May 2021; Accepted 20 May 2021
Available online 24 May 2021

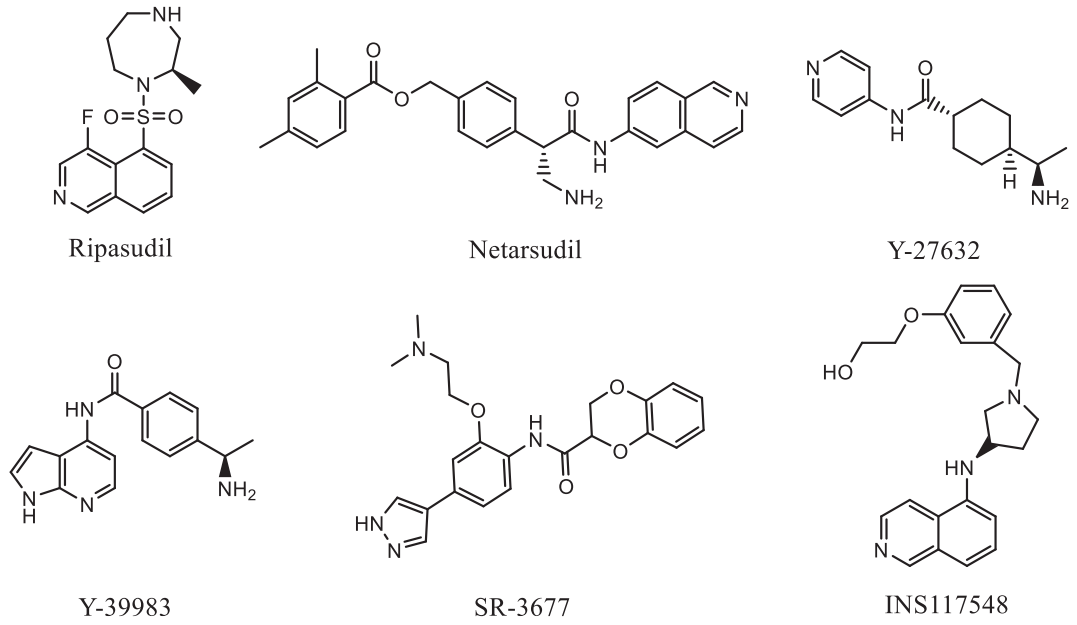

Fig. 1. Structures of representative ROCK inhibitors for anti-glaucoma.

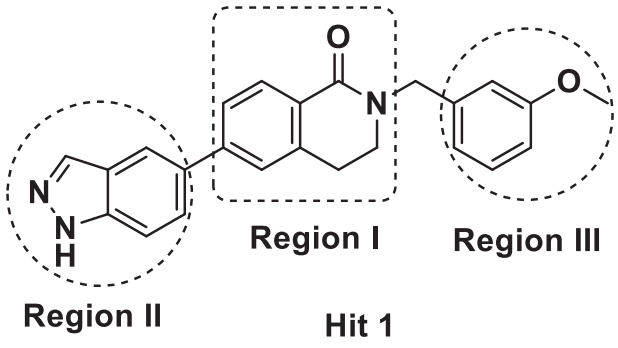

ROCK I: IC_{50} = 2.062 ± 0.103 μM

ROCK II: IC_{50} = 0.632 ± 0.059 μM

Fig. 2. The chemical structure of **Hit 1** together with regions (I, II and III) that are the focuses for the structure–activity relationship analysis.

coupling of **4** with commercially available reagent **5** produced final product **6**. Schmidt rearrangements were carried out on commercially available reagents **7a-c** to give intermediates **8a-c**. Suzuki-Miyaura coupling of intermediates **9a-c** obtained from nucleophilic substitution reaction of **8a-c** provided final compounds **10a-c**.

The kinase inhibitory activities of these compounds are given in Table 1. Replacement of the 3,4-dihydroisoquinolin-1(2*H*)-one moiety with benzo[*e*][*1,3*]oxazin moiety (**6**) improved the potency slightly. Expansion of the ring of **Hit 1** (**10a**) by inserting a methylene led to a decrease in potency for both ROCK I and II inhibition, while the same ring expansion of **6** (**10b**) resulted in slight and 3-fold increase in the ROCK I and ROCK II inhibitions, respectively. Introduction of two methyl groups to the 2-position of **10b** caused a decrease in ROCK inhibitory activity.

In the second step, we optimized region II with region I fixed as the optimal fragment 3,4-dihydrobenzo[*f*][1,4]oxazepin-5(2*H*)-one and region III as its original subgroup. A total of eight compounds were prepared. Scheme 2 shows the synthesis routes of compounds **12a-g** and **16**. Intermediate **9b** was coupled with different boronic acids or pinacol boronate esters through Suzuki-Miyaura coupling to give desired compounds **12a-g**. Intermediate **14** was obtained from 6-bromochroman-4-one (**13**) through Schmidt rearrangement. **14** was then treated with 3-methoxybenzyl bromide and sodium hydride in dry THF to give **15**. Finally, the desired product **16** was obtained through Suzuki-Miyaura coupling of **15** with pyridin-4-ylboronic acid.

Table 2 summarizes the chemical structures and ROCK inhibitory activities of these compounds. Replacement of 1*H*-indazole in **10b** with 1,3-benzodioxol (**12a**) led to the loss of activity. While 4-pyridine replacement (**12b**) made a significant increase to the ROCK inhibitory activity. However, compound **16** with 7-position pyridine substitution

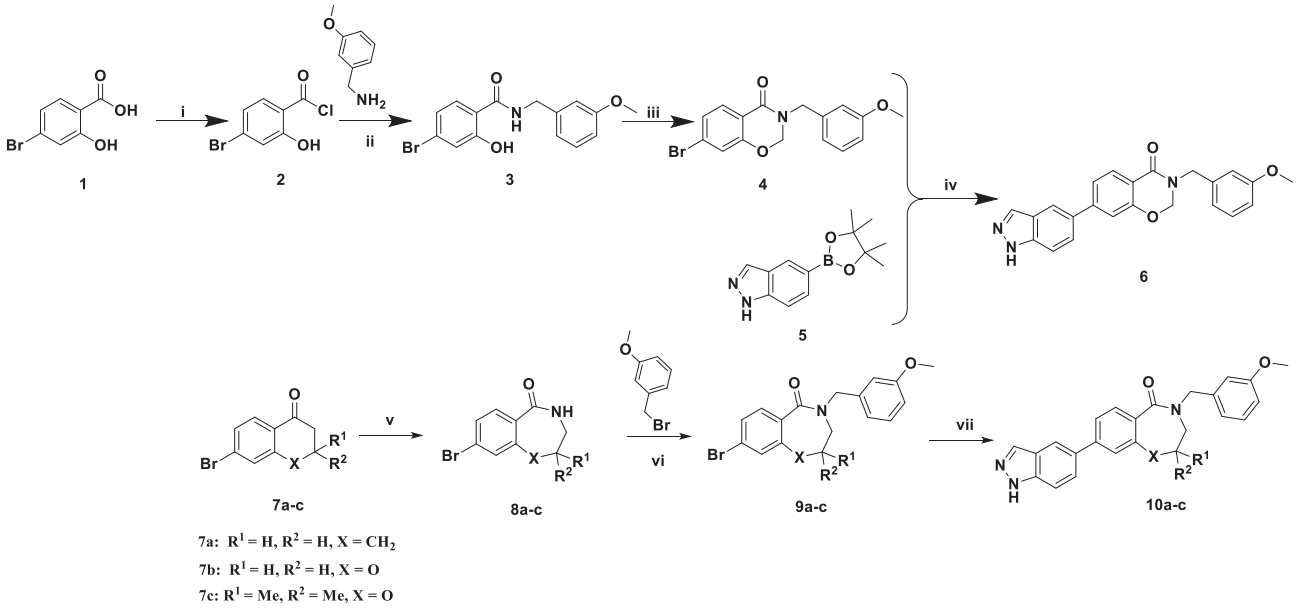

Scheme 1. Synthesis routes of compounds **6** and **10a-c**. Reagents and conditions: (i) $SOCl_2$, DMF, 85 °C, 5 h; (ii) TEA, THF, 25 °C, 8 h, 80%; (iii) Dibromomethane, Cs_2CO_3, MeCN, 80 °C, 24 h, 40%; (iv) $Pd(PPh_3)_4$, K_2CO_3, 1,4-dioxane/H_2O (10/1), N_2, 100 °C,10 h, 50%. (v) NaN_3, Methanesulfonic acid, DCM, 25 °C, 70–85%. (vi) NaH, dry THF, 0 to 50 °C, 4 h, 75–90%; (vii) $Pd(PPh_3)_4$, K_2CO_3, 1,4-dioxane/H_2O (10/1), N_2, 100 °C, 12 h, 55–58%.

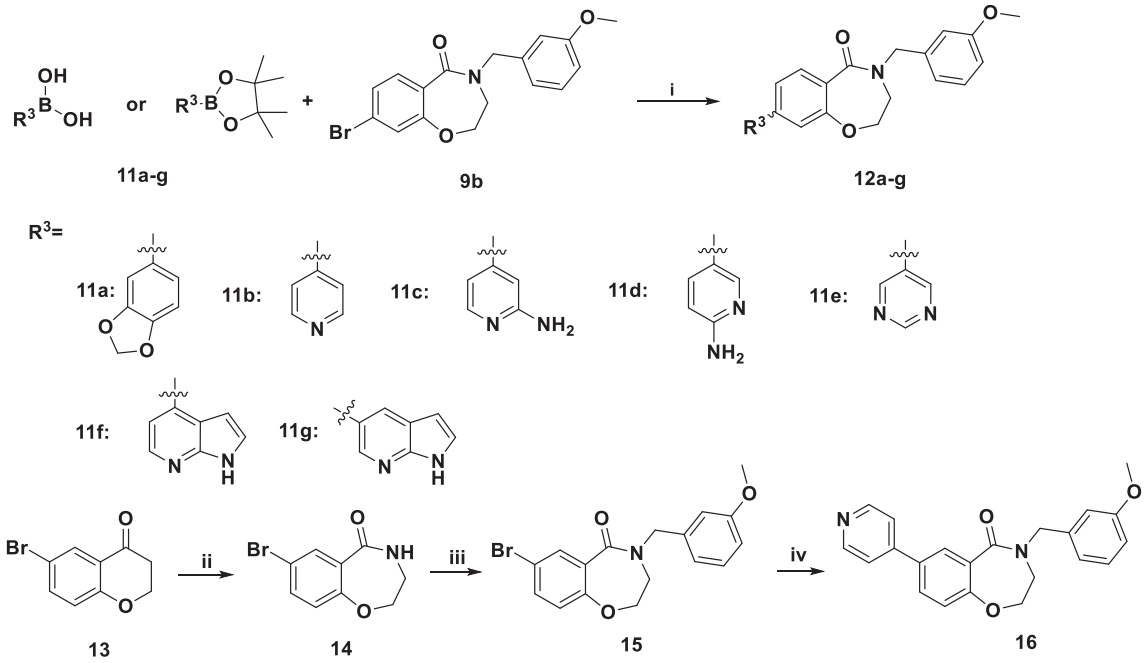

Scheme 2. Synthesis routes of compounds **12a-g** and **16**. Reagents and conditions: (i) 1,4-dioxane/water (V/V = 5/1), $Pd(PPh_3)_4$, Cs_2CO_3, 100 °C, 12 h; (ii) DCM, NaN_3, CH_3SO_3H, 0 °C to 25 °C, 12 h; (iii) dry THF, 1-(bromomethyl)-3-methoxybenzene, NaH, 0 °C to 25 °C, 12 h; (iv) 1,4-dioxane/water (V/V = 5/1), pyridin-4-ylboronic acid, $PdCl_2(dppf)\cdot CH_2Cl_2$ adduct, Cs_2CO_3, 100 °C, 12 h.

decreased ROCK inhibitory activity. An amino-substitution at 2-position (**12c**) resulted in a decrease in potency compared with **12b,** and further position adjustment of nitrogen and amino led to a loss of activity (**12d**). Pyrimidine replacement in region II also resulted in a loss of potency (**12e**). Finally, we replaced the 4-pyridine with azaindole, and the potencies of the resulting compounds (**12f** and **12 g**) did not exceed that of **12b**.

In the third step, region III was optimized with region I and II fixed as their optimal groups. We synthesized six compounds (**19a-f**). The synthesis of these compounds is shown in Scheme 3. Suzuki-Miyaura coupling of pyridin-4-ylboronic acid (**11b**) with various 4-benzyl-8-bromo-3,4-dihydrobenzo[*f*][1,4]oxazepin-5(2*H*)-one derivatives (**18a-f**), which were obtain from substitution reactions of **8b** with various commercially available benzyl bromide (**17a-f**), afforded final

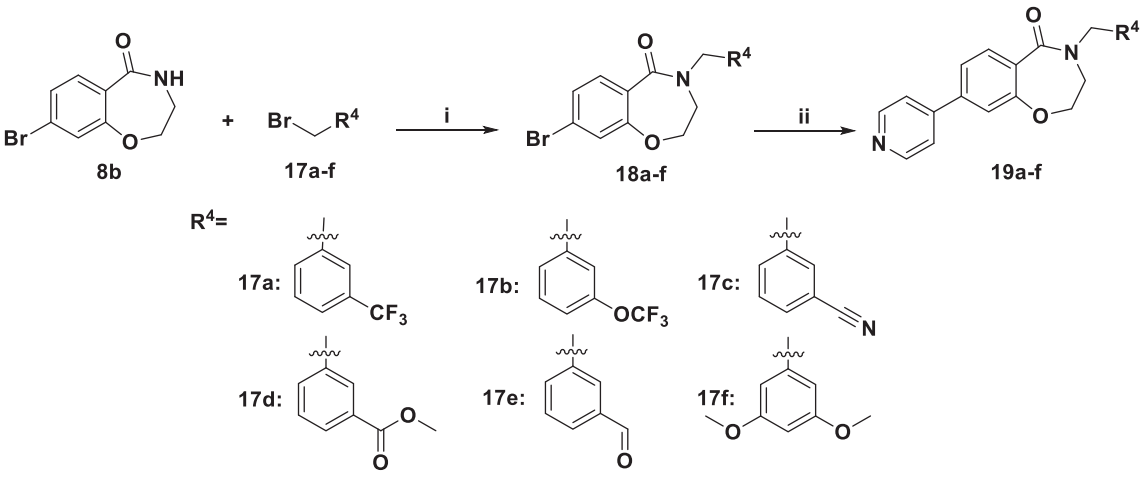

Scheme 3. Synthesis routes of compounds **19a-f**. Reagents and conditions: (i) DMF, NaH, 0 °C to 25 °C, 12 h; (ii) 1,4-dioxane/water (V/V = 5/1), pyridin-4-ylboronic acid, $Pd(PPh_3)_4$ or $PdCl_2(dppf)\cdot CH_2Cl_2$ adduct, Cs_2CO_3 or K_2CO_3, 100 °C, 12 h.

Table 1
Structures and *in vitro* biological activities of compounds **Hit 1**, **6** and **10a-c**.

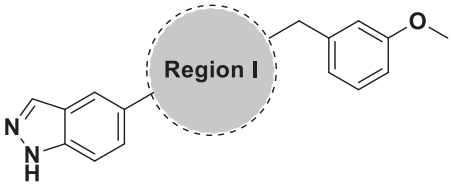

Compound	Region I	IC_{50} (μM)[a]	
		ROCK I	ROCK II
Hit 1	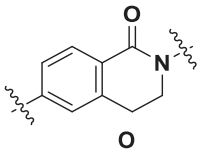	2.062 ± 0.103	0.632 ± 0.059
6	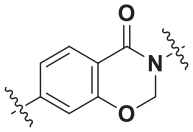	1.462 ± 0.099	0.434 ± 0.012
10a	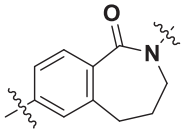	> 10	2.115 ± 0.087
10b	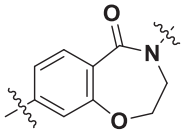	1.080 ± 0.150	0.182 ± 0.002
10c	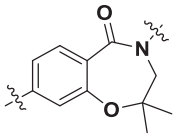	6.012 ± 0.260	0.749 ± 0.023

[a] IC_{50} values were determined from Kinase Profiler of Eurofins. The data are averages of two independent experiments reported as the mean ± SD.

compounds **19a-f**.

Table 3 shows chemical structures and ROCK inhibitory activities of compounds **19a-f**. Compared with the 3-methoxy substitution of phenyl in **12b**, other substituents at 3-position (**19a-e**) did not improve the potency against ROCK I and II. Adding another methoxy moiety at 5-position also decreased the activity.

The above structural optimization and SAR analyses led to the discovery of a number of compounds that showed potent activity against both ROCK I and ROCK II. **12b** is the most active compound. Further studies to this compound including kinase selectivity, binding mode prediction, and anti-glaucoma activity, will be carried out in the follows.

To examine the kinase selectivity, we tested the kinase inhibition profile of **12b** at a fixed concentration of 10 μM. Here 100 representative kinases were selected. The inhibition rates of **12b** against the selected kinases are shown in Table S1. Fig. 3 displays the human kinome dendrogram based on the measured inhibition rates. **12b** exhibited a high inhibition rate against only one kinase LIMK2 except ROCK I and II; LIMK2 is the direct downstream kinase of the ROCKs. [11] The calculated selectivity scores, S (5), S (10) and S (20), are 0.029,0.049 and 0.069, respectively. All of these data indicate that **12b** is a good selective ROCK inhibitor.

Molecular docking was then used to predict the binding modes of **12b** with ROCK I and II (Fig. 4). The structures of ROCK I and II were taken from the RCSB Protein Data Bank (PDB entries: 6E9W for ROCK I, and 6ED6 for ROCK II). The two ROCK isoforms share 92% similarity in their amino acid sequence,[23] and their active pockets (the ATP-binding site) are very similar. As predicted by molecular docking, **12b** occupies the active pockets of ROCK I and II with the same pose and orientation. In both ROCK I and II, the nitrogen of pyridine of **12b** forms a hydrogen bonding interaction with the NH backbone of Met (Met156 in ROCK I, and Met172 in ROCK II) in the hinge region. In addition, the amide carbonyl of **12b** forms another hydrogen bonding interaction with Lys105 in ROCK I, and Lys121 in ROCK II. The only difference is that the oxygen atom of 3-methoxy group of **12b** forms the third hydrogen bonding interaction with Lys216 in ROCK II, but the same interaction does not be formed in ROCK I due to the unfavorable distance between the oxygen atom of 3-methoxy group of **12b** and Lys200 (corresponding to Lys216 in ROCK II). This could be used to interpret that **12b** has a higher inhibitory activity against ROCK II than ROCK I.

Table 2
Chemical structures and *in vitro* biological activities of compounds **10b, 12a-g** and **16**.

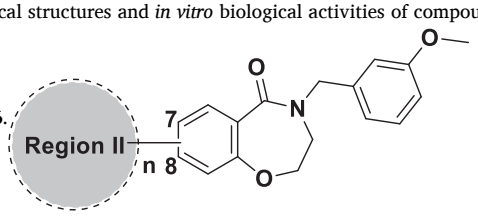

Compound	n	Region II	IC_{50} (μM)[a]	
			ROCK I	ROCK II
10b	8	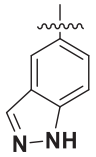	1.080 ± 0.150	0.182 ± 0.002
12a	8	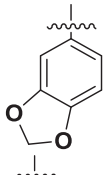	> 10	> 10
12b	8	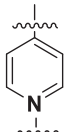	0.093 ± 0.004	0.003 ± 0.001
12c	8	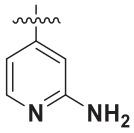	1.145 ± 0.107	0.015 ± 0.003
12d	8	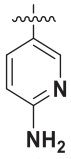	> 10	> 10
12e	8	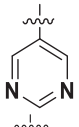	> 10	> 10
12f	8	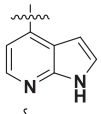	0.103 ± 0.026	0.015 ± 0.007
12g	8	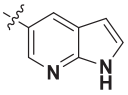	> 10	5.535 ± 1.102
16	7	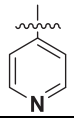	> 10	0.761 ± 0.096

[a] IC_{50} values were determined from Kinase Profiler of Eurofins. The data are averages of two independent experiments reported as the mean ± SD.

Western blot was then performed to determine the effect of **12b** on the ROCK signaling in intact cells. Here we detected the expression levels of MYPT1 and its phosphorylated form (p-MYPT1) in SH-SY5Y cell line[13]; MYPT1 is a direct downstream signal protein of ROCKs.[12] As shown in Fig 5, **12b** treatment dose-dependently inhibited the phosphorylation of MYPT1, but did not impact the expression of MYPT1. These results indicated that **12b** could efficiently suppress the ROCK signaling in intact cells.

Table 3
Chemical structures and *in vitro* biological activities of compounds **12b, 19a-f**.

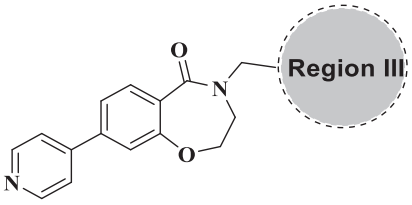

Compound	Region III	IC_{50} (μM)[a]	
		ROCK I	ROCK II
12b	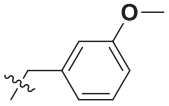	0.093 ± 0.004	0.003 ± 0.001
19a	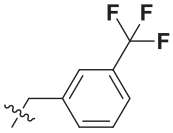	1.964 ± 0.621	0.133 ± 0.014
19b	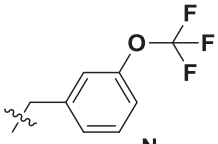	9.242 ± 1.209	0.495 ± 0.316
19c	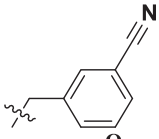	3.099 ± 0.202	0.050 ± 0.009
19d	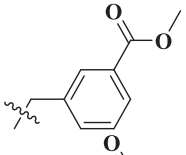	0.208 ± 0.004	0.009 ± 0.001
19e	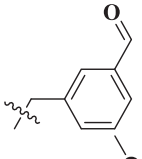	0.668 ± 0.125	0.029 ± 0.027
19f	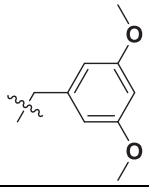	4.493 ± 0.039	0.217 ± 0.062

[a]IC50 values were determined from Kinase Profiler of Eurofins. The data are averages of two independent experiments reported as the mean ± SD.

Normotensive NZW rabbits were adopted to evaluate the IOP-lowering effect of **12b** *in vivo*. As shown in Fig. 6, comparing with vehicle, **12b** rapidly and significantly lowered IOP. The prominent IOP reduction was observed at 0.5 h after dose administration and was sustained for 2–3 h. The highest average IOP reduction was achieved at 1 h after instillation, and was 34.3% from baseline (4 mmHg). No obvious hyperemia was noticed during the course of the experiment, suggesting that **12b** could potentially separate the desired IOP-lowering effect of ROCK inhibitors from commonly observed side effect.

In summary, **12b** is a potent and selective ROCK inhibitor with a new chemical scaffold. It could efficiently lower IOP in normotensive NZW rabbits and did not show obvious hyperemia. Overall, **12b** is a good lead compound of anti-glaucoma and deserves further investigations.

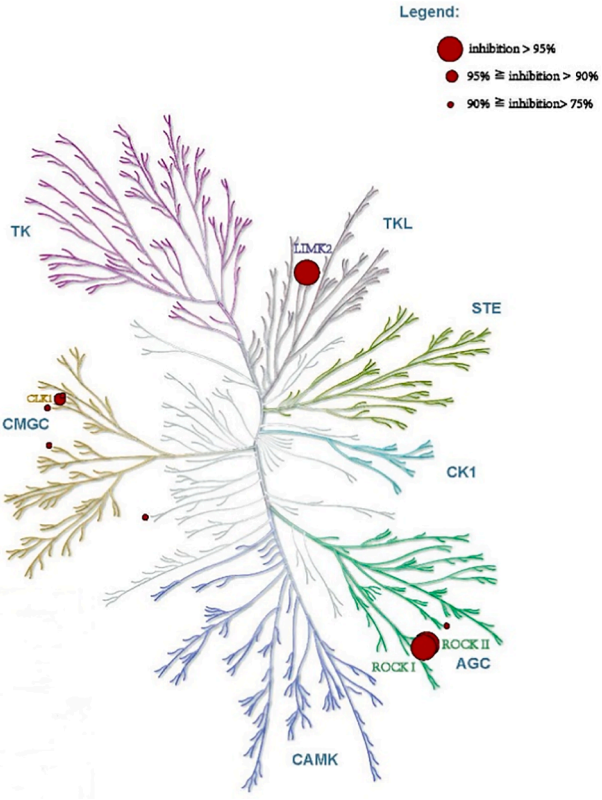

Fig. 3. The kinase selectivity of **12b** shown on the human kinome dendrogram.

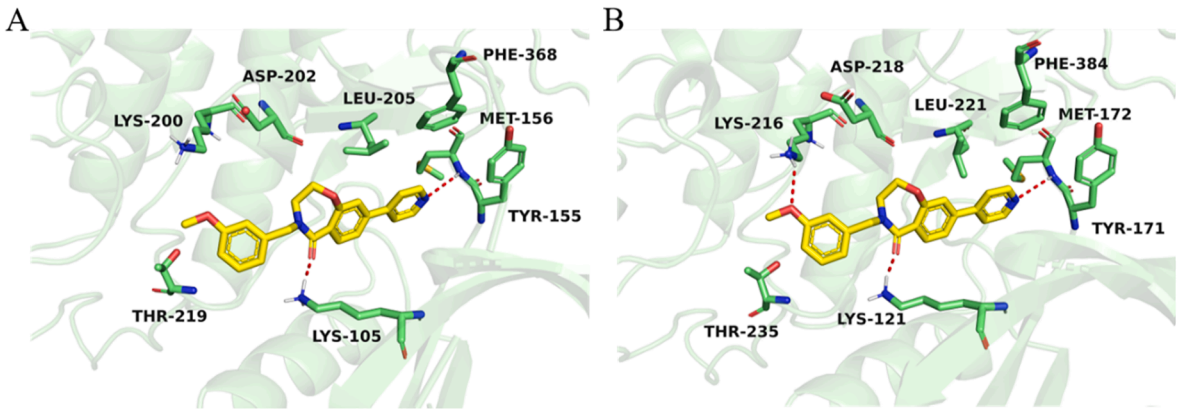

Fig. 4. Predicted binding modes of **12b** with ROCK I (A) and ROCK II (B). Dashed red lines indicate the hydrogen bonding interactions. The crystal structures of ROCK I (PDB entry: 6E9W) and ROCK II (PDB entry: 6ED6) were taken from the RCSB Protein Data Bank. (For interpretation of the references to colour in this figure legend, the reader is referred to the web version of this article.)

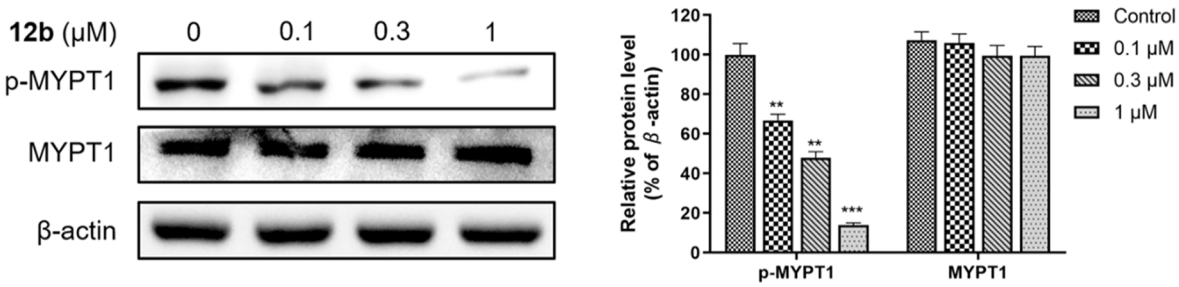

Fig. 5. **12b** reduced the level of p-MYPT1. SH-SY5Y cells were treated with various concentrations of **12b** (0.1, 0.3 and 1 μM) for 12 h. Quantification of immunoblots is presented in the right panel (* $P < 0.05$, ** $P < 0.01$, *** $P < 0.001$ vs. control, *t* test).

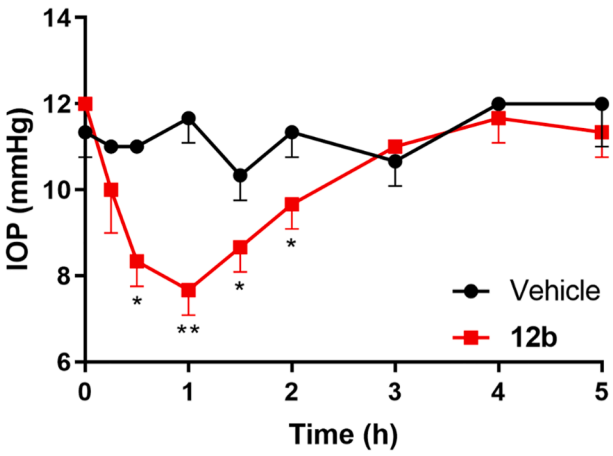

Fig. 6. IOP-lowering effects of the topical administration of 0.3% **12b** eye drops (red line) in one eye and the vehicle control in the other eye (black line) in ocular normotensive NZW rabbits. All data are expressed as the mean ± SD. (* $P < 0.05$, ** $P < 0.01$ vs. vehicle, *t* test). (For interpretation of the references to colour in this figure legend, the reader is referred to the web version of this article.)

Declaration of Competing Interest

The authors declare that they have no known competing financial interests or personal relationships that could have appeared to influence the work reported in this paper.

Acknowledgment

This work was supported by the National Natural Science Foundation of China (81930125, 81773633, and 21772130).

Appendix A. Supplementary data

Supplementary data to this article can be found online at https://doi.org/10.1016/j.bmcl.2021.128138.

References

1 Berrino E, Supuran CT. Rho-kinase inhibitors in the management of glaucoma. *Expert Opin Ther Pat.* 2019;29(10):817–827.
2 Tham Y-C, Li X, Wong TY, Quigley HA, Aung T, Cheng C-Y. Global prevalence of glaucoma and projections of glaucoma burden through 2040. *Ophthalmology*. 2014;121(11):2081–2090.
3 Braunger BM, Fuchshofer R, Tamm ER. The aqueous humor outflow pathways in glaucoma: a unifying concept of disease mechanisms and causative treatment. *Eur J Pharm Biopharm*. 2015;95:173–181.
4 Wei X, Cho K-S, Thee EF, Jager MJ, Chen DF. Neuroinflammation and microglia in glaucoma: time for a paradigm shift. *J Neurosci Res*. 2019;97:70–76.
5 Gagnon M-M, Boisjoly HM, Brunette I, Charest M, Amyot M. Corneal endothelial cell density in glaucoma. *Cornea*. 1997;16(3):314???318. https://doi.org/10.1097/00003226-199705000-00010.
6 Dikopf MS, Vajaranant TS, Edward DP. Topical treatment of glaucoma: established and emerging pharmacology. *Expert Opin Pharmacother*. 2017;18(9):885–898.
7 Schehlein EM, Robin AL. Rho-associated kinase inhibitors: evolving strategies in glaucoma treatment. *Drugs*. 2019;79(10):1031–1036.
8 Rao VP, Epstein DL. Rho GTPase/Rho kinase inhibition as a novel target for the treatment of glaucoma. *Biodrugs*. 2007;21(3):167–177.
9 Bandarage UK, Court J, Gao H, et al. ROCK inhibitors 4: Structure-activity relationship studies of 7-azaindole-based rho kinase (ROCK) inhibitors. *Bioorg Med Chem Lett*. 2021;33:127721. https://doi.org/10.1016/j.bmcl.2020.127721.
10 Green J, Cao J, Bandarage UK, et al. Design, synthesis, and structure-activity relationships of pyridine-based rho kinase (ROCK) inhibitors. *J Med Chem*. 2015;58(12):5028–5037.
11 Burridge K, Wennerberg K. Rho and Rac take center stage. *Cell*. 2004;116(2):167–179.
12 Kawano, Y. et al. Phosphorylation of myosin-binding subunit (MBS) of myosin phosphatase by Rho-kinase in vivo. J Cell Biol 147, 1023-1037 (1999).
13 Zhao L, Li Y, Wang Y, et al. Discovery of 4H-Chromen-4-one derivatives as a new class of selective rho kinase (ROCK) inhibitors, which showed potent activity in ex vivo diabetic retinopathy models. *J Med Chem*. 2019;62(23):10691–10710.
14 Zhang K, Zhang L, Weinreb RN. Ophthalmic drug discovery: novel targets and mechanisms for retinal diseases and glaucoma. *Nat Rev Drug Discovery*. 2012;11(7):541–559.
15 Abbhi V, Piplani P. Rho-kinase (ROCK) inhibitors – a neuroprotective therapeutic paradigm with a focus on ocular utility. *Curr Med Chem*. 2020;27(14):2222–2256.
16 Okumura N, Koizumi N, Ueno M, et al. ROCK inhibitor converts corneal endothelial cells into a phenotype capable of regenerating in vivo endothelial tissue. *Am J Pathol*. 2012;181(1):268–277.
17 Boland S, Bourin A, Alen Jo, et al. Design, synthesis, and biological evaluation of novel, highly active soft ROCK inhibitors. *J Med Chem*. 2015;58(10):4309–4324.
18 Garnock-Jones, Ripasudil KP. First global approval. *Drugs*. 2014;74(18):2211–2215.
19 Sturdivant JM, Royalty SM, Lin C-W, et al. Discovery of the ROCK inhibitor netarsudil for the treatment of open-angle glaucoma. *Bioorg Med Chem Lett*. 2016;26(10):2475–2480.
20 Hoy SM, Netarsudil SM. Ophthalmic solution 0.02%. *Drugs*. 2018;78(3):389–396.
21 Feng Y, LoGrasso PV, Defert O, Li R. Rho Kinase (ROCK) inhibitors and their therapeutic potential. *J Med Chem*. 2016;59(6):2269–2300.
22 Hsu C-R, Chen Y-H, Liu C-P, et al. A highly selective rho-kinase inhibitor (ITRI-E-212) potentially treats glaucoma upon topical administration with low incidence of ocular hyperemia. *Investigative Opthalmol Visual Sci*. 2019;60(2):624. https://doi.org/10.1167/iovs.18-25252.
23 Sharma P, Roy K. ROCK-2-selective targeting and its therapeutic outcomes. *Drug Discovery Today*. 2020;25(2):446–455.
24 Pan J, Yin Y, Zhao L, Feng Y. Discovery of (S)-6-methoxy-chroman-3-carboxylic acid (4-pyridin-4-yl-phenyl)-amide as potent and isoform selective ROCK2 inhibitors. *Bioorg Med Chem*. 2019;27(7):1382–1390.